UCRL-JC-133728
PREPRINT

Thermally-Induced Distortion of a High Average Power Laser System by an Optical Transport System

R. Chow
L. Ault
J. R. Taylor
D. Jedlovec

This paper was prepared for submittal to the
44th Annual Meeting of the International Symposium on
Optical Science, Engineering, and Instrumentation
Denver, Colorado
July 18-23, 1999

March 31, 1999

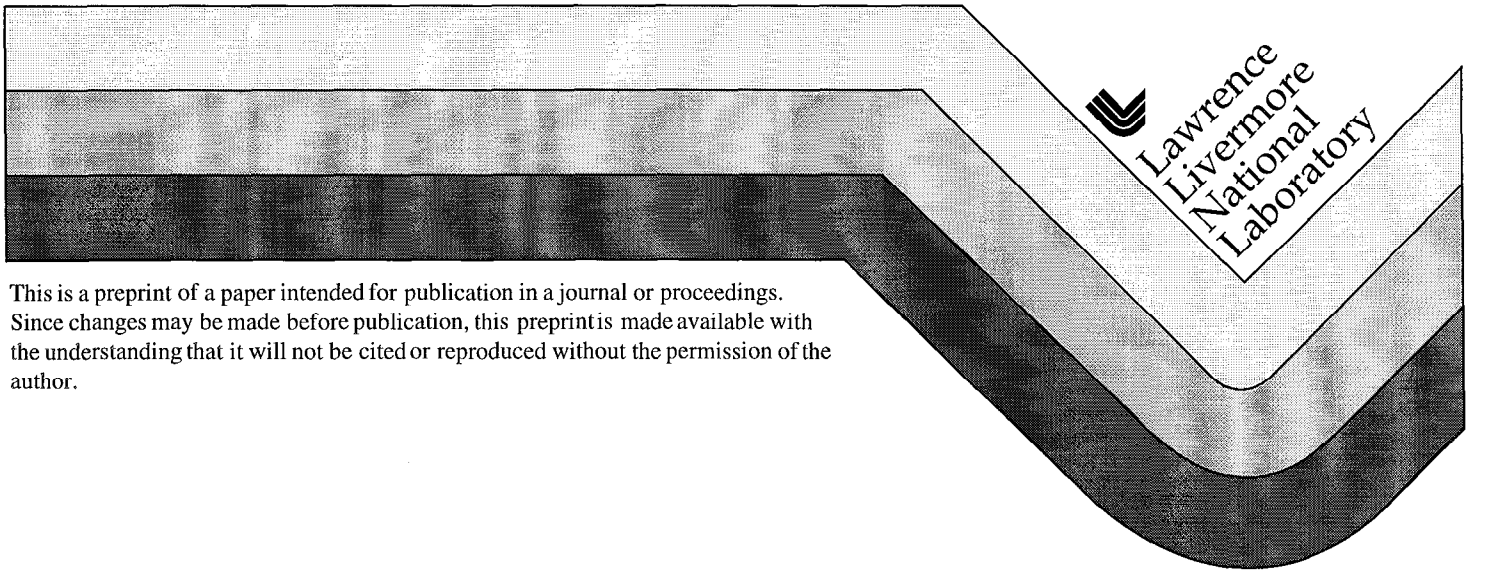

Thermally-induced distortion of a high average power laser system by an optical transport system

by Robert Chow [a], Linda Ault, John R. Taylor, and Don Jedlovec
Lawrence Livermore National Laboratory, Livermore, CA 94551

Key words: High power laser, absorptance, thermal lensing

Abstract

The atomic vapor laser isotope separation process uses high-average power lasers that have the commercial potential to enrich uranium for the electric power utilities. The transport of the laser beam through the laser system to the separation chambers requires high performance optical components, most of which have either fused silica or Zerodur as the substrate material. One of the requirements of the optical components is to preserve the wavefront quality of the laser beam that propagate over long distances. Full aperture tests with the high power process lasers and finite element analysis (FEA) have been performed on the transport optics. The wavefront distortions of the various sections of the transport path were measured with diagnostic Hartmann sensor packages. The FEA results were derived from an in-house thermal-structural-optical code which is linked to the commercially available CodeV program. In comparing the measured and predicted results, the bulk absorptance of fused silica was estimated to about 50 ppm/cm in the visible wavelength regime. Wavefront distortions will be reported on optics made from fused silica and Zerodur substrate materials.

1. Introduction

An uranium enrichment plant is projected to start operation by the year 2005 that utilizes atomic vapor laser isotope separation (AVLIS) technology. The AVLIS laser technology relies on a variety of high average power lasers that operate in a quasi-cw mode. The laser systems are designed to be of very high average power densities and beam quality in order to optimize enrichment efficiency. From the output of the amplifier chains through the enrichment area, each enrichment unit contains thousands of discrete optical transport elements distributed over considerable length (tens of meters) in a vacuum environment. These optical components are specified to stringent spectral requirements that include the ability to survive the high average laser power densities and to be low absorbing.

Low absorbing optical components are crucial to the economical viability of an AVLIS plant. Low absorptance coatings do not require active cooling and therefore lower the plant capital and operating costs. Wavefront quality is a key parameter in the propagation of laser beams over long distances since intensity uniformity affect the efficiency of the photo-ionization mechanism. Low absorptance optical components are required to boost the efficiency of the enrichment process by minimizing the wavefront distortions of the laser beams. These optics are used from the beginning of the light amplification dye laser systems and through to the end of the beam transport system where the atomic separation process takes place.

The purpose of these thermal tests was to quantify the heating effects on optical components by a high average power laser beam in the visible regime. Early analyses with high power lasers were done on infrared laser systems and therefore on different optical materials.[1,2] More applicable thermal analysis was reported using high average power, visible wavelength lasers.[3] However, the tests to verify the modeling used a small diameter beam at a very high power density, 49 kW/cm^2, on an uncoated fused silica substrate. In addition, the modeling concurrent with that effort assumed surface absorptances of the optics to be zero. As a closer replication of the plant design, thermal tests were done on the Laser Demonstration Facility which produces full-sized beams at plant power densities. Various optics were tested for susceptibility to heating by the process laser beam. Representative transport optics were modeled.

2. Modeling of thermal effects on optics

A large majority of the custom optics in the AVLIS system may be described as high reflectors on Zerodur substrates, leaker mirrors on fused silica substrates, and windows made of fused silica (Figure 1). These representative cases were modeled by finite element analysis (FEA) case with the Thermal-Structural-Optical (TSO) analysis code written at Lawrence Livermore National Laboratory.[4] The material parameters and dimensions of

typical fused silica and Zerodur optical components are listed in Table 1. The rectangular beam footprint is nominally 40 mm x 80 mm.

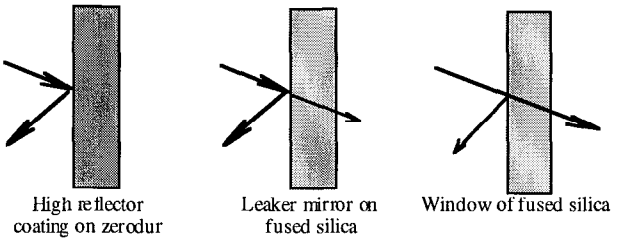

Figure 1 Examples of optical components in the AVLIS laser transport system.

Table 1 Material properties of fused silica and Zerodur in the TSO files.

Material Parameter	Units	Fused Silica Value	Zerodur Value
Diameter	mm	177.8	152.4
Thickness	mm	22.2	30.5
Density	g/mm^3	2.2 E-3	2.53 E-3
$\partial n/\partial T$	per °K	1.0 E-5	1.5 E-5
Specific Heat Capacity (C_p)	J/g K	7.5 E-1	8.21 E-1
Coefficient of thermal expansion (cte)	$°K^{-1}$	5.5 E-7	-7.0 E-8
Thermal conductivity (k)	W/mm K	1.4 E-3	1.64 E-3
Young's Modulus (E)	N/mm^2	7.3 E4	9.1 E4
Poison's ratio (ν)	dimensionless	1.7 E-1	2.4 E-1
Emissivity (= $E_{surface}$ * Stefan-Boltzman constant)	dimensionless	4.5 E-14	4.5 E-14

The wavefront is given as a Sag with units of waves at 647 nm. The Sag calculation to the first order is

$$\text{Sag} \approx H \tan(\delta)/\ 2\ /\ 647 \qquad \text{Eqn. (1)}$$

where H is the height of the marginal ray at the exit surface (Side 2 in Figure 2) defined by the beam footprint, and δ is the angle between the marginal ray and the exit surface. The Sag expression accounts for the different curvatures on sides 1 and 2 that operate on the marginal ray.

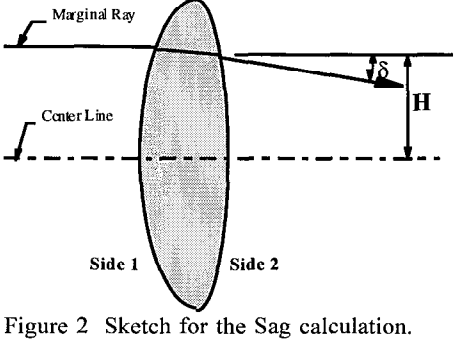

Figure 2 Sketch for the Sag calculation.

2.1. Fused silica modeling results

The transmitted wavefront distortions per kW of the window optic are plotted with bulk absorptances from zero to 100 ppm/cm, and surface absorptances from zero to 53 ppm. As absorptance increases in either case, the wavefront distortion per kW increases. The increase is larger in the Sag-Y direction than that in the Sag-X for the same conditions because the long axis of the rectangular beam coincides with the Sag-Y direction. When the window is heated by the laser beam, it becomes more like a lens. The two surfaces of the window becomes more convex due to differential thermal expansion coefficients and the refractive index increases with temperature. The modeling results indicate that neither surface nor bulk absorptance contributions can be neglected.

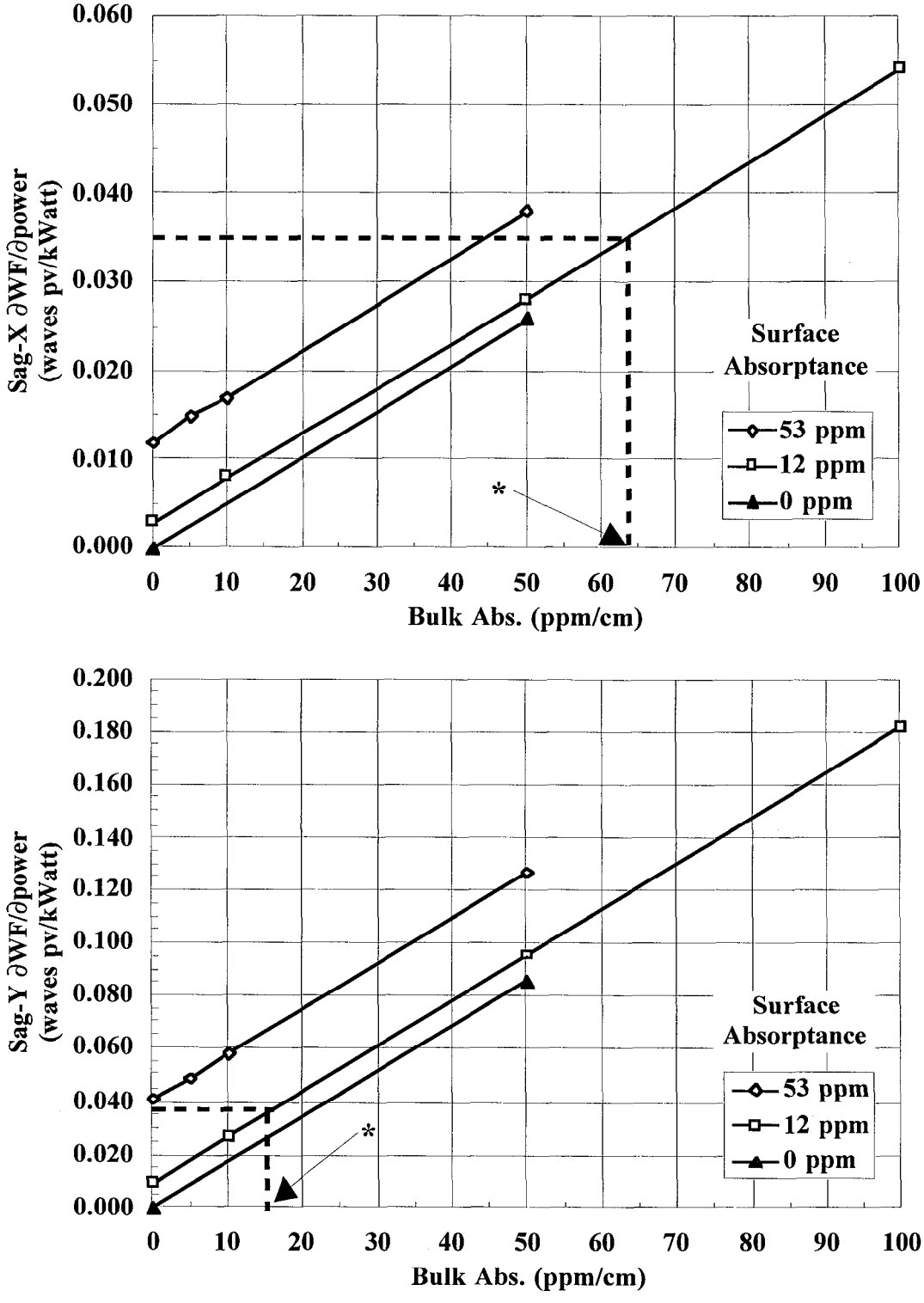

Figure 3a and b Finite element analysis of thermal-induced wavefront distortions on fused silica plano-plano window. Wavefront distortions along the 40-mm axis (Sag-X in Figure 3a) and the 80-mm axis (Sag-Y of Figure 3b) of the beam are shown as a function of surface and bulk absorptances. The window becomes like a focusing lens with increasing power or absorptance. *Estimated bulk absorptance of fused silica in the visible wavelength regime from on-line wavefront distortion measurements and modeling curves.

2.2. Zerodur substrate modeling results

Thermal effects of high reflector coatings, typically deposited onto Zerodur substrates, are reported in Table 2. The laser beam properties were identical to that used for the window analysis. The FEA analysis with 10 ppm surface absorptance (the specified coating absorptance) showed a thermal distortion thousands of times less than that predicted on a fused silica window. A high reflector with a "dirty" surface (100 ppm) still had a thermal distortions hundreds of times less than that of a fused silica window. The smaller distortions are attributed to the low thermal expansion coefficient of Zerodur material and the fact that the absorptance mainly occurs at the surface of the high reflector coating in contrast to the substrate and surface portions of a window.

Table 2 Thermal distortion comparisons between fused silica and Zerodur substrates. The fused silica window has 2 ppm surface and 10 ppm/cm bulk absorptances. A clean reflector coating on Zerodur had the specified 10 ppm of surface absorptance, and a dirty reflector coating on Zerodur had the 100 ppm of surface absorptance. The leaker mirror coating had the coating absorptance adjusted until the wavefront distortions were similar to that of the fused silica window.

Optical Component	Surface absorption (ppm)	Sag-X (over 40 mm)	Sag-Y (over 80 mm)
Window of fused silica	6	0.008	0.027
High reflector on Zerodur	10	1.75 E-6	3.71 E -6
High reflector on Zerodur	100	1.56 E-5	3.42 E -5
Leaker mirror on fused silica	200	0.010	0.023

2.3. Leaker mirror on fused silica modeling results

The thermal distortions from a leaker mirror on fused silica approach that of a fused silica window only when the optical coating is highly absorbing or dirty. The distortions are greater than that of the Zerodur optic because of higher thermal expansion coefficient of fused silica.

3. Experimental set-up

Three Diagnostic Hartmann Sensor (DHS) packages were deployed at various locations along the LDF laser beam transport path. A 0.5 watt Kr ion laser diagnostic beam was formatted into a 4 x 8 cm rectangular footprint and co-propagated with the high power laser beams. The probe beam is leaked through certain transport optics into the respective DHS systems. A video camera captures the images from a 72 lenslet array. The pixel images are archived and software-processed in a variety of methods. The data may be presented as a 3-dimensional rendering of the beam wavefront, and as wavefront sag, peak-to-valley (PV), and root-mean-square (RMS) values as a function of time.[5] The PV value is simply the maximum wavefront displacement found in a given image. The RMS calculation follows the standard deviation formula of the wavefront displacements about the average. The sag determination is more involved. A least-squares fit of the data is made to a parabolic function. The curve is rotated to eliminate the coefficient of the cross term (in other words, the principle axis are found). Finally, the sag is calculated from the product of the maximum X or Y value with the respective X^2 or Y^2 coefficients. The sag values proved to be most useful in determining wavefront changes due to thermal effects. There was too much noise in the PV time-trends and too small of a change in the RMS time-trends. Individual offsets in the packages are removed during the subtraction of wavefronts between the cold and hot condition of the optical transport system.

The dye lasers apply thermal loads of approximately 2 to 4 kW as determined by the calorimeters inserted at the end of each laser dye chain. The equilibration time for the optics to thermalize for both heat-up and cool-down is about 20 minutes (Figure 4). The type and number of optics between each DHS package is given in Table 3.

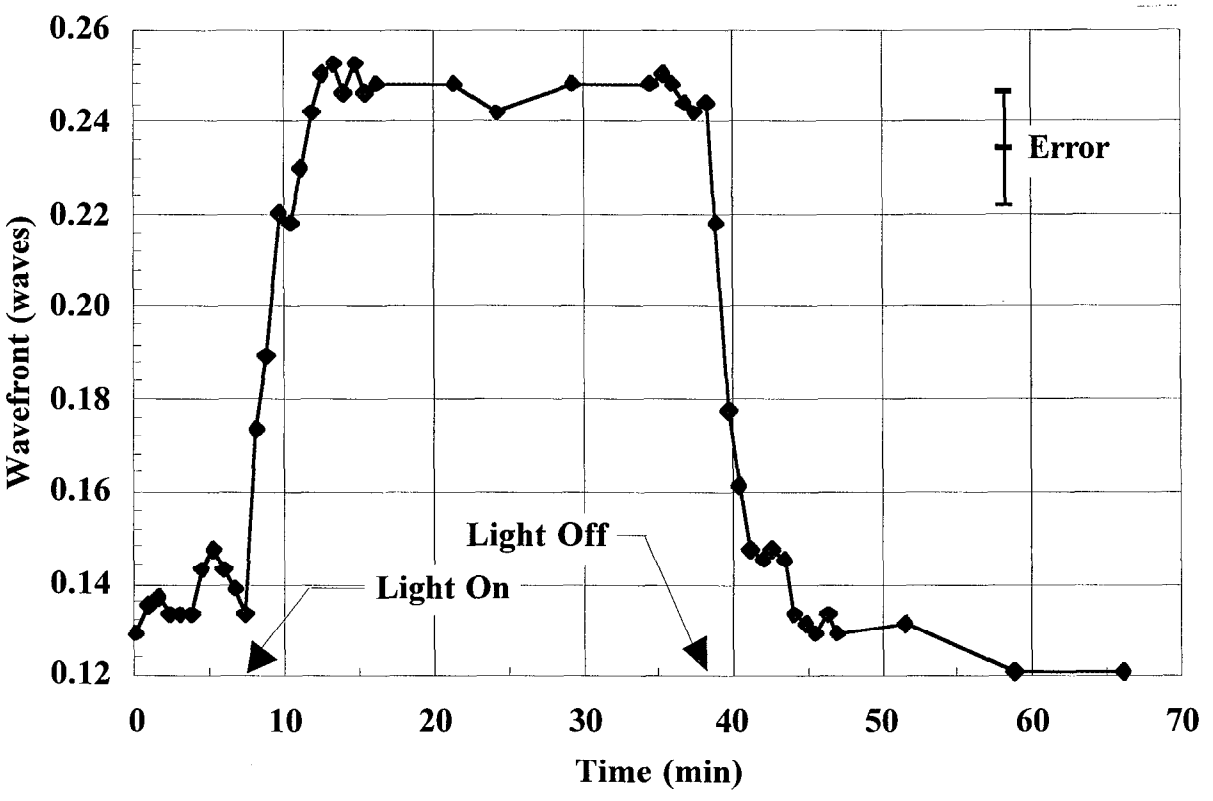

Figure 4 Heat up and cool down characteristics of the optical transport system at DHS package B.

Table 3 Optics quantity and type that are located between each DHS package. ZD = Zerodur; FS = fused silica.

DHS packages	Reflective ZD optics	Transmissive FS optics	Leaker FS optics
A to B	14	None	2
B to C	7	1	3

The optic of interest in this report is the transmissive optic between DHS packages B and C. The optic is a plano-plano fused silica window, coated on both sides with an anti-reflective coating at specified at 600±20 nm. The fused silica material is of grade "A" quality, specified with an homogeneity of 1 ppm, and a maximum bubble inclusion of 0.28 mm. The substrates are 177.8 mm in diameter by 22.2 mm thick. The optics are finished to a flatness of < 0.05 waves peak-to-valley in transmission.

4. Experimental Results

4.1. Thermal effects from the DHS packages

The experimental results plotted in Figure 5 confirms what the FEA modeling predicted, that the transport path with the transmissive optic would have the most distortion. The thermal-induced wavefront change at each DHS package is shown in Figure 5, where a positive change in wavefront indicates that the beams converge with increasing thermal loading. To remove power dependencies, the wavefront change due to thermal loading was divided by the power available for each test session.

The types of optics between each diagnostic package are provided to show which types optics contribute to thermally-induced wavefront distortions. There was no significant wavefront change between DHS packages A and B, indicating that up to 14 reflective and 2 leaker optics in series are not measurably affected by the thermal loads up to 4 kW. Then between the B and C DHS packages there is a measurable increase attributed to the presence of a transmissive optic in this transport path. The distortions contributed by leaker optics were discounted because no changes were measured between the DHS packages A and B.

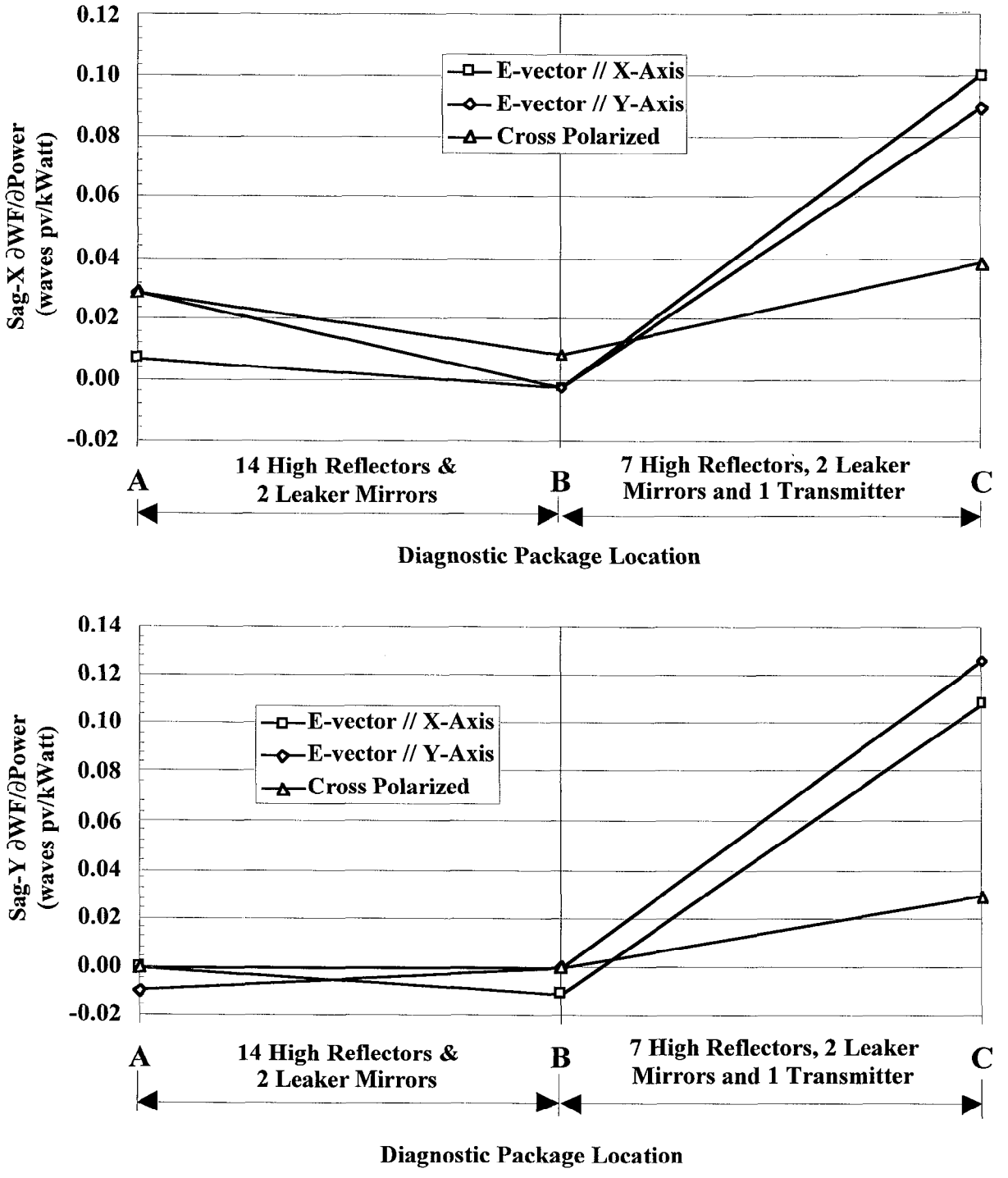

Figure 5 Thermally-induced wavefront distortions for single and cross polarized laser beams. The standard deviations of the measurements are discussed in a later section. The cross-polarized test was conducted with a clean window. The single-polarized tests were conducted with a window contaminated with oil.

At the power densities for the test, the thermal distortion were as small as 0.04 waves per kW of beam power. The transport path was re-configured with additional window locations as shown in Figure 6. In the modified configuration, other windows were deployed in a "2nd position", either in the insertable window mount or in a custom optics mount after the normal location. The additional window accentuated the thermal effect which made it

easier to measure the wavefront distortions. A number of windows were moved and switched amongst these three locations, and some windows were returned to their original positions in order to include variations caused by window installation. No significant data was obtained when three windows were tested together; the probe beam converged to a footprint smaller than that allowed to keep the DHS package operational. However, seven measurements were made with 2 windows in the beam path and the results given in Table 4. A 1-window result was derived from half of the 2-window average, 0.034 ± 0.005 and 0.037 ± 0.017 waves per kW for the Sag-X (40-mm) and Sag-Y (80-mm) directions, respectively.

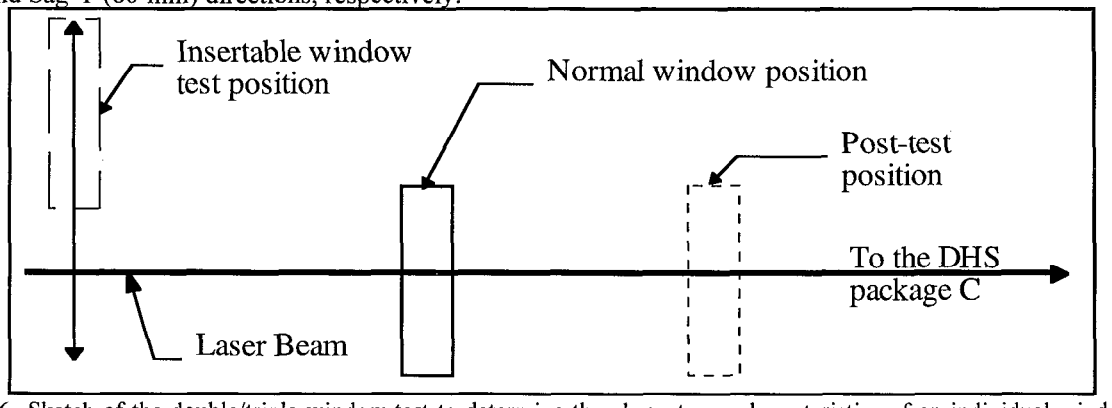

Figure 6 Sketch of the double/triple window test to determine the absorptance characteristics of an individual window and the standard deviation of the measurement.

Table 4: Double window tests. Sag values are given in waves per kW of the process beam. The 2nd position is a window optic either in the "insertable window" or the "Post-Test" position.

Location ->	Normal	2nd	Sag-X	Sag-Y
Window serial numbers	20	15	0.064	0.079
Window serial numbers	20	12	0.062	0.046
Window serial numbers	20	12	0.061	0.053
Window serial numbers	15	20	0.073	0.084
Window serial numbers	20	3	0.073	0.084
Window serial numbers	20	5	0.070	0.077
Window serial numbers	20	14	0.068	0.089
2-window Average			0.067	0.073
2-window Standard Deviation			**0.005**	**0.017**
1-window = 2-window Average divided by 2			**0.034**	**0.037**

The thermal distortions per power are nearly identical in both directions (Table 4 and Figure 5), in spite of the fact that the beam is twice as long as it is wide. According to FEA results in Figure 3, the distortion in the Y-direction should be ≈ 4x larger than that in the X-direction. In the FEA analysis, the power density is assumed to be uniform across the beam footprint. In reality, there is an estimated ±30% non-uniformity in the power density and the beam footprint is far away from the pupil plane at the DHS C-package. A possible method to improve the match between modeling and experiment may be to use a more accurate representation (size and intensity) of the laser beam in the TSO input file.

The standard deviations of DHS package A wavefront measurements are ± 0.015 and ± 0.010 waves/kW in the Sag-X and Sag-Y directions, respectively. The standard deviation was determined from a set of 6 measurements. The standard deviations of the DHS package B wavefront measurements are ± 0.014 and ± 0.005 waves/kW in the Sag-X and Sag-Y directions, respectively. The standard deviation was determined from a set of 12 measurements. The wavefront standard deviations are smaller for Sag-Y than Sag-X in these two packages because the thermal distortions in the Y-direction were very small, and the value of zero change was recorded in many cases.

4.2. Other wavefront effects

There are two other aspects of the data plotted in Figure 5. There appeared to be no differences in thermal effects between laser beams of different polarizations. However, the wavefront distortions between the single and cross polarization are different at the DHS C-location. During initial testing in the single window configuration, this large thermal effect at the C DHS package was noted. The installed window was inspected carefully with a bright light source and both sides of the optic were found contaminated. The contaminant could not be removed with a simple solvent wipe but was removed by soaking for a few days dilute in room-temperature acetic (CH_3OOH) solution. Since the contaminant appeared to be thicker at the edges than at the center, the contaminant may have been excessive or residual vacuum grease on the O-ring. After cleaning, the spectral trace and small laser beam testing showed that the part met spectral and laser survivability requirements. Interestingly, the off-line absorptance testing[6] of the contaminated and cleaned optical surfaces could not differentiate between the clean and contaminated conditions of the optic. The surfaces had absorptances of 14 ppm on side 1 and 39 ppm on side 2. In order to avoid laser damage to the part, the absorptance testing was performed only on the outer edges of the coating, away from the clear aperture, and in the area contacted by the O-ring. This test area had the heaviest concentration of vacuum grease and may still have retained some residual contamination that affected the low level absorptance test. The on-line thermal test appears to be a much more sensitive test of absorption and contamination than that of the off-line small beam test.

4.3. Bulk absorptance

The average wavefront distortion obtained from Table 4 was used in Figure 3 to estimate the bulk absorptance of fused silica at the visible wavelength regime. The intersection (dotted lines) of the measured Sag-X and Sag-Y wavefront distortions to the 12 ppm surface absorptance line puts the fused silica bulk absorptances between 15 to 64 ppm/cm. This data is in the first row of Table 5 along with the prior efforts to determine absorption and thermal effects of transmissive optics in the visible wavelength regime. The first two rows utilize the combination of wavefront distortions with high power density beams on transmissive optics and TSO.

The bulk absorptance estimated from this work falls in the wide range gathered from the literature, 1.0 to 140 ppm/cm. The literature data are listed in Table 5. The wide range of bulk absorptance values may be attributed to the various material quality of the fused quartz samples tested, and some spread may even be attributed to the measurement technique. In the former case, those that mentioned samples as Suprasil-quality fused silica had tested different grades of Suprasil. In the latter case, the photothermal deflection (PTD) appeared to have high resolution compared to calorimetry and the thermally-induced wavefront techniques. Not only are the absorption data reported with higher precision, the PTD technique was able to differentiate between Corning and Suprasil material which the calorimetry technique could not in ref. 8. The PTD bulk absorptances are even lower than that reported from the other techniques even though the PTD pump wavelength was shorter (and physically the material should have a higher absorptance). The large variations of fused silica bulk absorptances from the literature indicates that further work is needed in absorptance measurements and procedures. A calibrated standard for low loss tests of bulk and surfaces of optical components would benefit the optics community.

Table 5 Comparison of thermal-induced wavefront distortions and bulk absorptances. Abs = absorptance; NA = not applicable or assessed; WF = wavefront distortion with high power laser beam and TSO analysis; Cal = calorimetry by laser pump source; PTD = photothermal deflection with a laser pump source

Ref.	Author	Ave. Sag (Waves/kW)	Bulk Abs (ppm/cm)	Wave-length (nm)	Laser beam footprint (cm)	Ave power density (kW/cm^2)	Test	Material tested
Now	Chow	0.035	15 to 64	600	4 x 8	0.12	WF	Corning 7940
3	Cohen	0.060	5	600	0.13 ø	49	WF	Corning 7940 & Dynasil
7	Mori	NA	30	600	0.02 ø	< 16	Cal	Suprasil W1
8	Swimm/ Bass	NA	10 ± 5	600	NA	NA	Cal	Suprasil-2 & Corning 7940
9	Harrington	NA	140 ± 30	514	NA	NA	Cal	Generic fused silica
10	Strain	NA	1.0 ± 0.4	514	0.008 ø	19.9	PTD	Suprasil 312
10	Strain	NA	6.0 ± 1.6	514	0.008 ø	19.9	PTD	Corning 7940

5. Conclusions

Thermally-induced distortions were measured for a high power laser operating in the visible wavelength regime. Transmissive optics made of fused silica are the dominant contributors to thermal distortions in an optical transport system of an high average power laser. The wavefront distortion per kW is 0.034 ± 0.005 and 0.037 ± 0.017 in the Sag-X (40 mm) and Sag-Y (80 mm) directions, respectively. Leaker mirrors on fused silica and high reflector on Zerodur are did not contribute measurable wavefront distortions when irradiated with thousands of watts of process laser power. The thermal effects are independent of process beam polarization.

Bulk absorptances of 15 to 64 ppm/cm were derived by combining the measurements with the FEA behavior of fused silica. The wide spread in the values is probably due to the assumption of a uniform beam intensity over a rectangular footprint.

Auspices

This work was performed under the auspices of the U. S. Department of Energy by Lawrence Livermore National Laboratory under Contract W-7405-Eng-48.

References

1. H. E. Bennett, "Thermal distortion thresholds for optical trains handling high pulse powers," NBS **SP 462**, pp. 11-24, 1976.
2. J. S. Loomis and E. G. Bernal, "Optical distortion by laser heated windows," NBS **SP 435**, pp. 126-142, 1975.
3. S. J. Cohen, R. E. English Jr., C. J. Stolz, and J. R. Taylor, "Thermal analysis of transmissive elements in high average power laser beam delivery systems," SPIE **1992**, July 19-24, San Diego, UCRL-JC-110937.
4. TSO is a software code written to interface CODEV, TOPAZ3D (Arthur B. Shapiro, *A 3-dimensional finite element heat transfer code*, UCID-20484, Aug. 1985), and NIKE3D (J.O. Halliquist, *An implicit, finite-deformation, finite element code for analyzing the static and dynamic response of 3-dimensional solids*, UCID-18822, Jan. 1981).
5. J. T. Salmon, E. S. Bliss, J. L. Byrd, M. Feldman, M. A. Kartz, J. S. Toeppen, B. Vanwonterghem, S. E. Winters, "An adaptive optic system for solid-state laser systems used in inertial confinement fusion," SPIE **2633**, 1st annual international conference on solid state lasers for applications to ICF, Monterey, CA, 31-May to 2-June, 1995, pp. 105-113.
6. C. R. Stolz, J. R. Taylor, T. Sarginson, "Damage test capabilites using a high-repetition rate visible laser at LLNL," in Laser-induced damage in optical materials: 1991, SPIE **1624**, pp. 109-115.
7. H. Mori and T. Izawa, "A new loss mechanism in ultralow loss optical fiber materials," *J. Appl. Phys.* **51**(4), pp. 2270-227, April 1980.
8. R. T. Swimm, Y. Xiao and M. Bass, "Calorimetric study of optical absorption of Suprasil W-1 fused quartz at visible, near-IR, and near-UV wavelengths," *Appl. Optics* **24**(3), pp. 322-323, 1 Feb 1985.
9. J. A. Harrington, B. L. Bobbs, M. Braunstein, R. K. Kim, R. Stearns, and R. Braunstein, "Ultraviolet-visible absorption in highly transparent solids by laser calorimetry and wavelength modulation spectroscopy," *Appl. Optics*, **17**(10), pp. 1541-1546, 15 May 1978.
10. K. A. Strain, J. Hough, N. A. Robertson, K. Skeldon, "Measurement of the absorptance of fused silica at $\lambda = 514.5$ nm," *Optics Comm* **117**, pp. 385-388, 1995.

[a] Correspondence: Lawrence Livermore National Laboratory, Mail Stop 7000 East Ave., L-463, Livermore, CA 94551, 925-422-7615, chow3@llnl.gov

Back page stamp: Chow, pg. , SPIE 3782-27 for SD14, Stahl, Optical Manufacturing and Testing III